Configurable Design Approach for Heavy-duty Vehicle Powertrain Design

Isa Banagar*, Tommi Huhtala, Juho Könnö* and Amin Mahmoudzadeh Andwari
Machine and Vehicle Design (MVD), Materials and Mechanical Engineering, Faculty of Technology, University of Oulu, 90014 Oulu, Finland.

*Corresponding author(s). E-mail(s): juho.konno@oulu.fi; and isa.banagar@oulu.fi

Abstract

The design and fine-tuning of propulsion systems are facing significant challenges, considering the importance of maximizing energy efficiency and reducing carbon emissions. As internal combustion engines (ICEs) no longer exclusively control powertrains for heavy-duty vehicles (HDVs), the advent of emerging technologies in electrified powertrains and energy systems has presented a wide range of choices. None of the available concepts can satisfy all the requirements in different use case scenarios without compromising performance and energy efficiency. However, the number of available concepts for the powertrain increases the design flexibility while simultaneously elevating the challenge of design complexity. System-level simulation has provided great opportunities to predict system functionality at the very early stages of design. Considering a hybrid powertrain that includes different subsystems, simulation blocks representing each subsystem should be developed to predict the system behavior precisely. In this study, a configurable design approach is developed addressing the design complexity of an integrated e-axle in a truck use case. Different simulation methods for different subsystems of the powertrain are investigated, and a generic simulation structure is proposed for configurable simulations. Simulations of the subsystems are developed by cooperating with suppliers using different simulation tools. To implement a clear interface between the simulations, based on the generic structure of a hybrid powertrain with an e-axle, simulations for the different systems in the form of functional mockup units (FMUs) have been proposed. The simulations are separately compared against available measured data from a test truck with a conventional powertrain and suppliers' data to be validated. After validation, different configurations of the system, component sizing, and different control strategies are investigated for driving cycles acquired from fleet owners to design the suitable system for the final use case scenario.

The Authors declare that we prefer to include the paper in the conference proceedings.

Keywords: Configurable design, Hybridization, Electrification, Heavy Duty Vehicle

Internal Combustion Engine	ICE
Functional Mock-up Unit	FMU
System Structure and Parametrization	SSP
Functional Mock-up Interface	FMI
Machine and Vehicle Design	MVD
Equivalent Circuit Model	ECM
Original Equipment Manufacturer	OEM
State of Charges	SoC

Table 1. List of abbreviations

1 Introduction

The consumption of fossil fuels and the resulting environmental degradation have greatly propelled the advancement and adoption of sustainable design approaches. The primary source of greenhouse gas emissions in the US is power generation (25%) and transportation (28%)[1], making power generation and propulsion systems a crucial target for reducing energy consumption and pollution. Internal combustion engines (ICEs) have been the main component of propulsion systems for many years. Remarkable advancements have taken place in various aspects of powertrain design, which enhance their efficiency but increase their design complexity. Advanced propulsion systems are composed of diverse energy conversion, and energy storage systems such as ICEs, fuel cells, regenerative systems, and batteries [2], [3], [4], [5]. Moreover, there are other systems that interact with the power generation systems to enhance the overall efficiency of the system, i.e., vehicle control systems and

advanced driving assistant systems [6]. Although the mentioned technological interaction and advancement may improve efficiency, and flexibility, and reduce environmental effects, they increase design complexity[7]. The share of heavy-duty vehicles (HDVs) is 9% in the global vehicle fleet and 17% in total vehicle driven miles. Considering the environmental impact of road transport, 39% of the life-cycle road vehicle greenhouse gas emissions are produced by HDVs, among which trucks with more than 15-ton weight represent 75% of carbon dioxide emissions. Global truck freight activity is estimated to double between 2015-2050, which emphasizes HDVs' powertrain improvement either by means of novel fuel or alternative fuel and energy sources[8], [9].

Vehicle system-level simulations demonstrate great capability for decision-making in terms of powertrain architecture definition for hybrid HDVs. Hybridization of HDVs as a solution for emission reduction required a precise trade-off between fuel consumption, payback period, cost, weight, packaging, and emissions as well as optimized component selection and sizing [10]. Salek et al. [11], optimized the battery and fuel cell capacity of a hybrid powertrain for a class 8 HDV by developing vehicle system-level model via AVL cruise M and optimizing the powertrain parameters with a genetic algorithm. The same approach has been studied for the size of the battery for a full electric powertrain [12].

Each engineering domain has its own preferred design and analysis methods and tools. This means that a single system can be modeled using multiple tools, each providing a distinct but often overlapping perspective. While it might be possible to manage all relevant views within a tool offered by a single vendor for certain applications, in other cases, this approach may neither be practical nor preferable, especially at the early stages of design. Standardization of the simulation in the form of a functional mock-up unit (FMU) can facilitate the simulation process, especially in the concept development phase, by providing the capability of performing co-simulation utilizing black-box simulations, which could be generated in different simulation tools[13]. To simulate complex systems using FMUs, a modular approach could be employed wherein separate FMUs represent individual subsystems. This allows for the independent simulation and validation of each subsystem and provides flexibility in configuring the final system. For instance, different variations of the same subsystem, such as the battery in a hybrid powertrain, can be tested against a consistent set of other subsystems. By adopting this approach, the interactions between different systems can be investigated by subsystem providers without sharing confidential model parameters or know-how of simulations, which facilitates identifying the most optimal configurations. To standardize the interfaces for FMUs in co-simulations and facilitate broader adoption, the System Structure and Parametrization (SSP) standard has been introduced as an extension to the Functional Mock-up Interface (FMI) standard. SSP serves as a tool-independent format for developing and exchanging connections between simulations in a co-simulation environment. This standardization enhances interoperability and simplifies the process of integrating FMUs from different sources, streamlining the co-simulation workflow, and promoting collaboration in product development and within the research community[14].

A robust base simulation framework is essential for identifying interactions between different components and defining interfaces of FMUs. In this study, we developed a basic simulation framework for a conventional 8x4 truck. Initially, the simulation was calibrated using a set of measured data to ensure accuracy and reliability. Subsequently, electric components of the hybridized powertrain were added to the model. The developed simulation facilitated the investigation of interactions between component sizing effects and design parameters. Identifying these interactions is essential to refine the simulation framework and prepare the foundation for defining the interfaces of FMUs in subsequent stages of the research.

2 Method

In this section, a simulation setup to predict vehicle fuel consumption is described. The model is organized into separate components within a generic simulation framework. This simulation setup has been developed to facilitate the assessment of different component configurations and their interdependencies. This approach will enable a comprehensive exploration of vehicle design options, leading to enhanced fuel efficiency and cost optimization.

For the mathematical calculation of vehicle dynamics and energy consumption, the AVL Cruise M 2022 has been utilized. Its built-in capability of making separate simulations for different components makes it one of the best options to develop base simulations for each component of the vehicle. Initially, a model of the nominated truck with a conventional powertrain has been developed and verified against measurements. Subsequently, individual component models have been developed for electric subsystems of the hybridized powertrain, to form a generic model of a hybridized HDV. Then interactions between systems have been investigated via developed simulation. In the following sections, we provide brief descriptions of each component model, offering insight into their characteristics and contributions to the overall simulation framework.

For vehicle longitudinal dynamics calculations, the vehicle module of cruise M has been utilized. It calculates the dynamic forces of road inclination, rolling resistance, acceleration, deceleration, aerodynamic forces, drivetrain loss, and dynamic wheel loads. In this study, the research truck of the Machine and Vehicle Design (MVD) research group has been modeled using the presented values in Table 2. The nominated truck is a SISU Polar

DK12M with an 8x4 axle configuration and a total load capacity of 18.7 tons. It is produced by the Finnish heavy vehicle manufacturer Sisu Auto, equipped with a Mercedes-Benz OM 501 V6 diesel engine and a 16-speed manual gearbox. Overall engine and gearbox characteristics [15], [16] have been mentioned in Table 1. Mentioned tire rolling resistance provided by the tire manufacturer according to ISO 28580. A coastdown test has been done to compute the drag coefficient. A higher drag coefficient compared to those reported in the literature [17] has been calculated from measurement data, which suggests a thorough analysis of test procedures, equipment, and conditions. According to ISO 28580 standard procedure, the tire rolling resistance value is calculated after the tire warms up, in controlled thermal conditions on an ideal road surface. Differences between the coastdown measurement condition and the standard measurement condition cause an underestimation of rolling resistance in the calculation compared to the real condition. Wind speed and angle are other effecting parameters while calculating driving resistance forces, which cannot be measured with the measurement setup. In the absence of wind data and different road surface conditions and different tire temperatures compared to the standard measurement condition, the aerodynamic drag coefficient is higher to calculate a similar driving resistance force compared to the coastdown measurement. The constant velocity test [18], considering the moment of inertia of rotating components, deviation of rolling resistance at different temperatures, and a better vehicle warm-up procedure according to the Vecto-approach [18], are identified as solutions to fine-tuning and accurate dedication of driving resistance forces to resistance sources. The driveline efficiency has been selected as 0.94 for each gear mechanisms, using the range of values mentioned for different base-line vehicle in the literature[17].

Truck specifications	Distance from hitch to front axle [mm]	6920
	Wheelbase [mm]	4700
	Curb weight [kg]	14300
	Total Load capacity [kg]	18700
	Gross weight (including the max. payload) [kg]	33000
	Axle configuration	4x2 and 8x4
Aerodynamic parameters	Frontal area [m^2]	7
	Drag coefficient	1.15
Tire parameters	Rolling resistance steering axles [N/kN]	7
	Rolling resistance driving axles [N/kN]	6.2
Engine specifications	Type	V6 engine with one exhaust-gas turbocharger and charge-air intercooling
	Displacement [cm^3]	11946
	Max. Power [kw]	350
	Max. Torque [N.m]	2300
	Valve	4 valves
	Compression ratio	1:17.75
	Emission Legislation	Euro V
Transmission specifications	Type	Automated manual transmission
	Gear ratios	11.7 – 0.68
	Rear axle ratio	3.6
	Wheel-hub gear reduction ratio	1.18
	Gearbox efficiency	0.94
	Final drive efficiency	0.94
	Wheel-hub gear reduction efficiency	0.94

Table 2 vehicle general specification

The P4 hybrid configuration without plug-in charging capability has been selected as the targeted hybrid vehicle configuration. This configuration has been selected due to MVD's objectives of developing a modular hybrid powertrain for further research and practical constraints. Specifically, this configuration offers flexibility and requires minimum modifications to the current powertrain. The schematic of the hybrid powertrain of the truck has been depicted in Figure 1. As it can be seen from the schematic the e-axle including a battery module, motor, and 2-speed gearbox, which are added as the second driven axle.

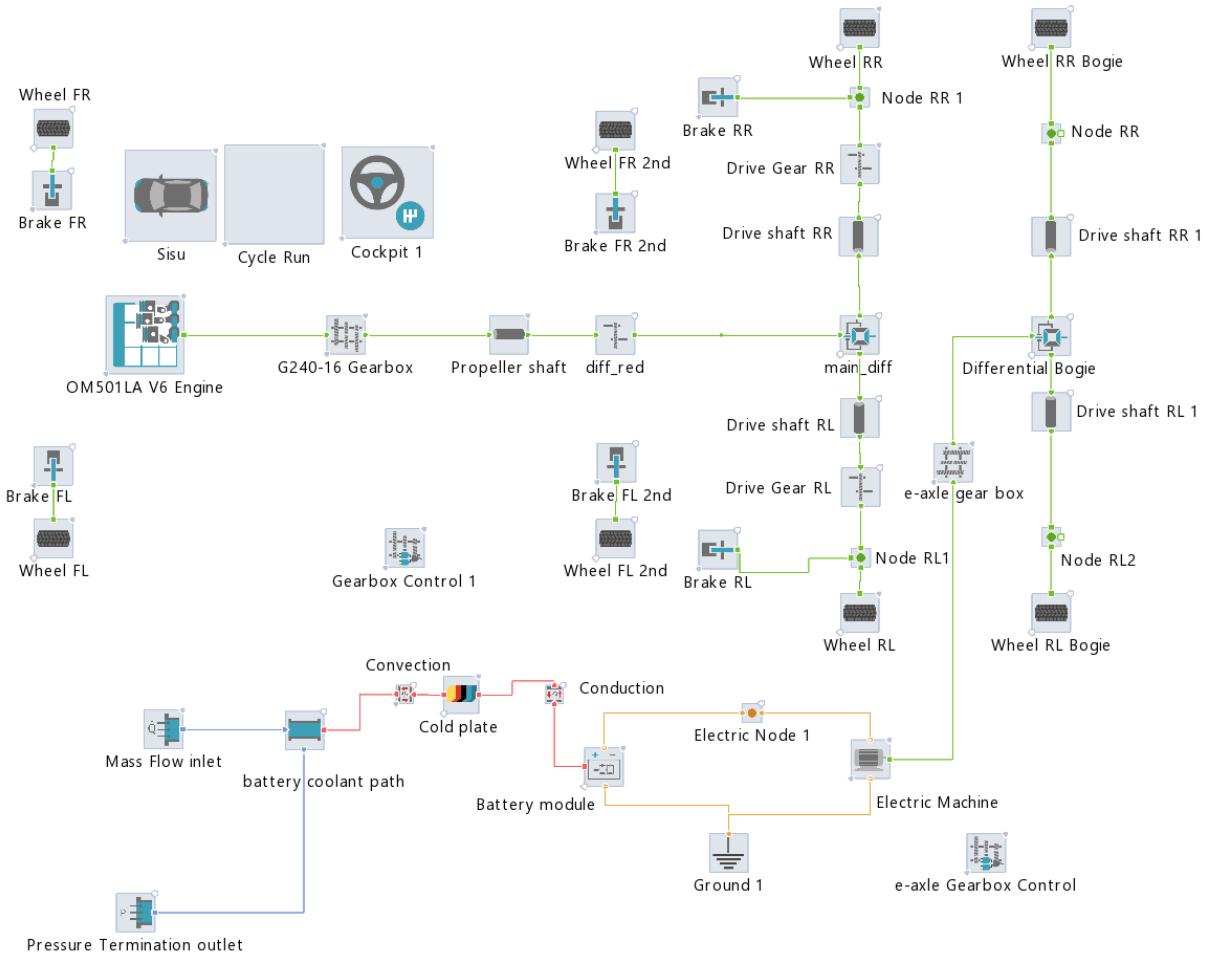

Figure 1, Vehicle powertrain configuration.

To evaluate the accuracy of the simulation, the simulated fuel consumption of the 4x2 configuration of the vehicle, lifted auxiliary steering, and driven axle, without load has been compared against measured data from the same setup. The engine speed for upshifting and downshifting has been set to 1300 rpm as 800 rpm in the simulation. To ensure identical gear shifting in simulation and measurement, these values have been given as instructions to the driver during measurement to have the same engine operational condition in simulation and measurement. Measured data of a 430 km round trip of the second driving cycle in Table 4 has been utilized for simulation and model verification and vehicle parameters have been set based on the given values in Table 2. The simulation calculates 34.4 l/100km fuel consumption, which shows an acceptable 5.8% overestimation compared to 32.5 l/100km recorded from vehicle CAN data.

After the evaluation of the base simulation of the conventional vehicle, the e-axle component has been parametrized using the parameters mentioned in Table 3. The battery parameters have been chosen based on proposed specifications for HDVs' high-voltage batteries, with additional consultation with the Original Equipment Manufacturer (OEM) to determine the parameters for an Equivalent Circuit Model (ECM). The ECM model employs resistance and capacitance networks to characterize the battery's electrical behavior across varying states of charge (SoC) and operational temperatures. The model includes a simplified thermal model for the battery that calculates the battery temperature by considering the battery's internal resistance and generated heat and battery material thermal coefficients. Therefore, it predicts the average temperature in the battery and does not consider the temperature difference in different locations of the battery module. The specific values of these parameters are not disclosed due to confidentiality reasons, the simulation results have been validated by the OEM.

To explore the impact of battery capacity on overall efficiency, two configurations were considered for simulation: a single battery pack with a capacity of 15 kWh, and a dual-series battery pack with a capacity of 30 kWh. For motor simulation, the available model from the Cruise M library was utilized due to a lack of a valid dataset. However, it's important to note that adding an inverter simulation to the available motor dataset is essential to enhance the accuracy of the simulation. Same as the conventional powertrain gear shifting strategy, 4000 rpm for upshifting and 500 rpm for downshifting have been defined as shifting points of the 2-speed gearbox.

Battery Specifications	Capacity [kWh]	15
	Voltage [V]	780
Motor	Max. Torque [N.m]	882 (0 to 2700 rpm)
	Max. Speed [rpm]	6000
Gear box	1st gear ratio	30.17
	2nd gear ratio	13.21

Table 3. E-axle specification

To examine the effects of operational conditions two driving cycles have been selected, Table 4. The first driving cycle data has been selected from a fleet owner dataset to investigate the proposed hybrid system for this specific use case. The second driving cycle data has been measured with the introduced MVD's research vehicle and has been utilized to calibrate the vehicle model parameters. The first driving cycle features frequent uphill and downhill, while in contrast, the second driving cycle begins with road segments characterized by uphill and downhill sections, transitioning to a nearly flat road for the second half of the trip. Moreover, the first driving cycle is entirely uphill, whereas the second is entirely downhill. These distinctions in road elevation and the difference between the two driving cycles have been chosen to investigate the influence of operational conditions on system design. The driving cycles velocity profiles acquired from vehicles without loads. For a more realistic simulation, the velocity profile should be defined for each load condition, since simulating these driving cycles for the full load condition causes unrealistically high fuel consumption due to their high average speed. This approach enables us to assess the dynamics of various driving conditions and their effects on vehicle performance and fuel consumption. The velocity profile and road altitude profile have been represented in Figure 2, and Figure 3.

Parameter	First driving Cycle	Second driving cycle
Distance	108 (km)	215 (km)
Max Speed	92 (km/h)	90 (km/h)
Avg Speed	73.5 (km/h)	77.66 (km/h)

Table 4 Driving cycles characteristics.

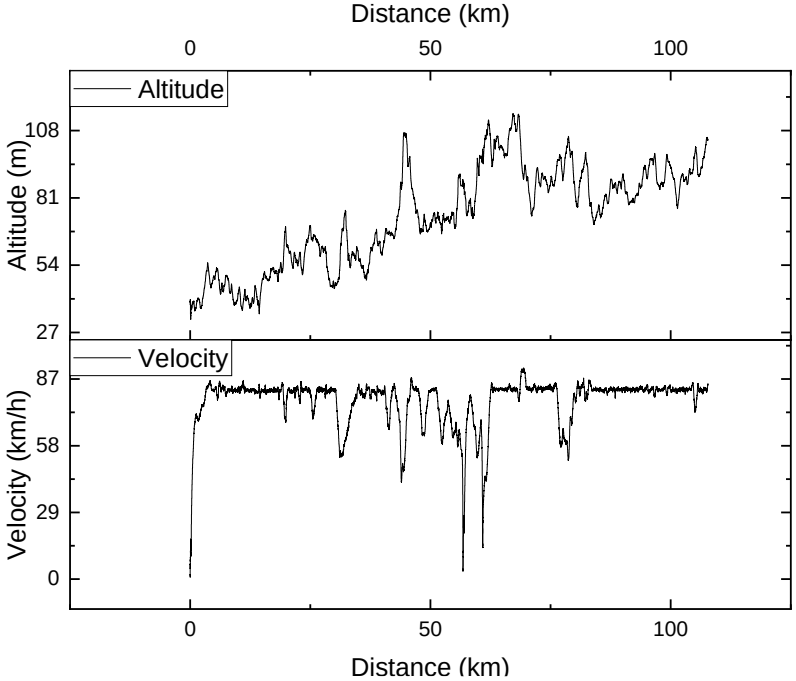

Figure 2.First driving cycle.

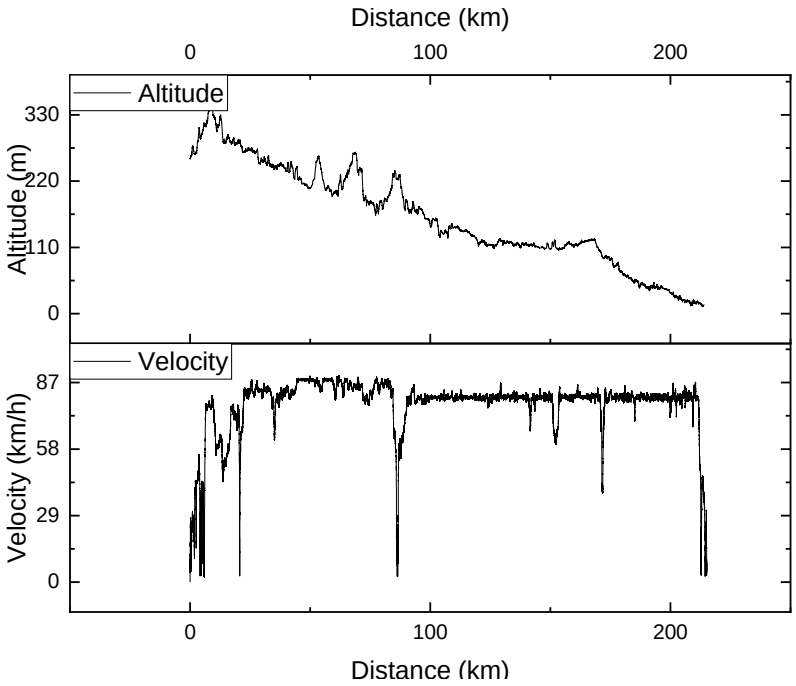

Figure 3.Second driving cycle.

A rule-based control strategy is the most common method to control the energy flow of a hybrid powertrain. The parameters of a rule-based strategy should be calibrated and optimized for the best performance in a variety of operational conditions. In this study, a deterministic rule-based control strategy has been utilized to investigate the influence of the control strategy on fuel consumption. The target is to study the sensitivity of selecting a suitable control strategy and the effect of its threshold values on sizing other components, not to determine the best control strategy. The logic of the rule-based strategy has been depicted in Figure 4. Boost mode, charging mode, and e-axle switched off are defined as three operational modes of the e-axle. If the accelerator pedal position exceeds the pedal position threshold, the vehicle velocity does not exceed the velocity threshold, and the battery charge is not below the SoC threshold, the boost mode will be turned on. Similarly, the charge mode will be turned on when the brake pedal position exceeds the pedal threshold, vehicle velocity is above the defined threshold, and the battery charge is less than the SoC threshold. In both modes, the motor's torque is equal to the multiplication of the motor's maximum torque and the position of the pedal in percentage. Vehicle velocity thresholds define engagement regions of the e-axle, such as urban or highway areas. The SoC threshold for the battery limits the battery usage due to safety and durability concerns. Moreover, the accelerator and brake pedal position thresholds dictate the frequency and intensity of the e-axle engagement. While high pedal threshold values limit the engagement of the e-axle to high-demand acceleration or deceleration situations, with lower values, the e-axle engages more frequently.

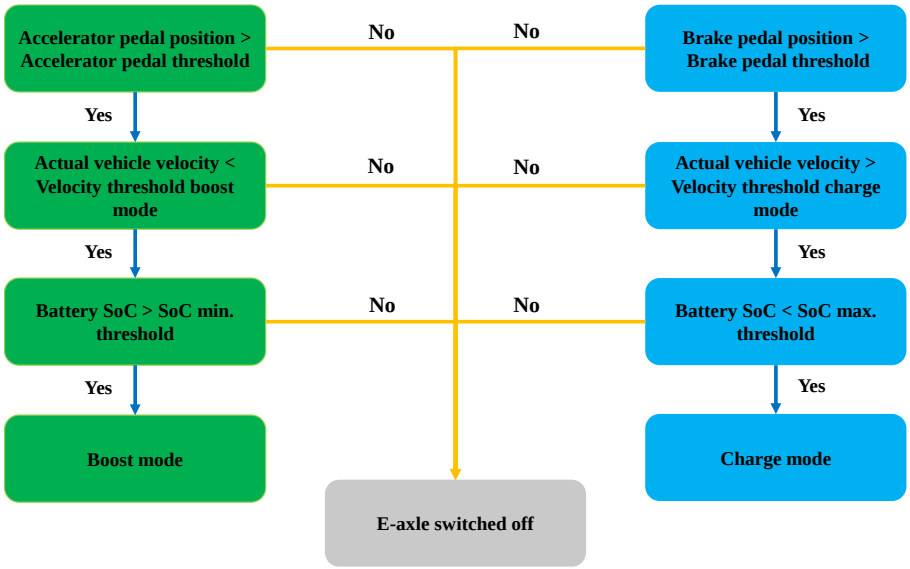

Figure 4, Rule-base strategy schematic.

3 Result

The parameter study for the hybrid powertrain has been conducted using the two mentioned driving cycles. Each driving cycle has been subjected to two scenarios: the empty scenario, representing driving without load, with a gross weight of 14.3 tons, and the full load scenario, with a full load capacity of 33 tons gross weight. This comprehensive approach enables a thorough examination of the vehicle's behavior across a range of operating conditions. To explore the impact of battery pack capacity, two battery pack capacities, as mentioned previously, each initialized with a 50% SoC, have been considered. SoC thresholds for the battery pack were determined in consultation with the OEM, set at 80% for the maximum SoC and 20% for the minimum SoC. Since speed limit for the urban area is 60 km/h and is 80 km/h for highway, these limits have been utilized to identify the urban and highway regions in the driving cycles. The vehicle velocity thresholds parameter of the control strategy is set at 50 km/h and 70 km/h. These values restrict the e-axle engagement to urban areas with the first value and enabling the possibility of engagement of it in all driving conditions except road and highway cruising with the second value. The velocity threshold for the charging mode is set at 25 km/h for all simulation cases. To investigate the sensitivity of pedal thresholds, a range of 20% to 80% of pedal engagement has been considered for both acceleration and brake pedals, with 20% intervals for acceleration pedal values and 15% intervals for brake pedal values. In total, five values for brake pedal thresholds, four values for accelerator pedal thresholds, two vehicle velocity thresholds, two battery capacities, and two load scenarios have been selected for each driving cycle. The thermal simulation of the battery system has been done to ensure the battery operates within its designated temperature limits in the absence of an e-axle torque limiter. Without the torque limiter, the e-axle motor can be operated out of its' defined continuous torque region longer than it could operate in real condition, which leads to e-axle's electric motor and battery overheating. Analyzing the battery thermal simulation is beyond the scope of this study, and the results were only utilized to eliminate scenarios with extreme power demand, which leads to extreme thermal conditions. For the parameters mentioned, no critical cases have been identified. The results of the simulations have been discussed.

A total of 320 simulation cases have been run for the mentioned parameters. To perform a parameter study, vehicle fuel consumption has been selected as an identifier value. However, to develop an optimal control strategy and the selection of the best components, factors like powertrain overall efficiency, end-of-cycle SoC, and cost should also be considered, which are not in the scope of this study.

Figures 5 and 6 show the variation of fuel consumption in each driving cycle against control threshold values of accelerator pedal position, brake pedal position, and vehicle velocity. Each graph includes 80 dots representing fuel consumption for one set of battery capacity, velocity threshold, accelerator pedal threshold, and brake pedal threshold. Different values of vehicle velocity thresholds in the boost mode are differentiated through color coding, with thresholds of 50 km/h displayed in purple and 70 km/h displayed in cyan.

According to the results, fuel consumption is highly sensitive to the vehicle velocity threshold value. Since both driving cycles are motorway-dominated, restricting the e-axle engagement to urban areas with a velocity threshold of 50 km/h led to higher fuel consumption for both scenarios and cycles. This limitation resulted from the e-axle's engagement being confined to a small fraction of the overall cycle. Moreover, considering the dashed lines as an overall trend of fuel consumption variation, it is more sensitive to the accelerator pedal threshold compared to the brake pedal threshold in the empty scenario, Figure 5 (b) and Figure 6 (b). On the other hand, in the full load scenario, fuel consumption has less sensitivity to the accelerator pedal threshold and more sensitivity to the brake pedal threshold compared to the empty scenario. For the first driving cycle, minimum fuel consumption in the full load scenario is achieved by accelerator pedal thresholds ranging from 0.2 to 0.6, Figure 5(c). In contrast, minimum fuel consumption for the second driving cycle and the same scenario only achieved by a 0.2 acceleration pedal thresholds, Figure 6 (c) and Figure 6 (d), which demonstrates the effects of operational conditions on the tuning of control strategies.

For the first driving cycle, the best fuel consumption has been achieved by multiple pedal threshold values both for empty and full load scenarios. For the empty scenario, the least fuel consumption is achieved by a 0.2 accelerator pedal threshold and a 0.65 brake pedal threshold. However, the fuel consumption value for the same accelerator pedal position and other brake pedal thresholds is almost the same, Figure 5 (b), which causes different end-of-cycle SoC, Figure 7. Moreover, the same happens with the acceleration pedal position for the full load scenario in Figure 5(c). The least fuel consumption is achieved by a 0.2 accelerator pedal threshold and a 0.2 brake pedal threshold. Almost same fuel consumption is simulated with different accelerator pedal thresholds, which define the intensity of charge depletion, and the case with a lower pedal threshold consumes the battery charge faster, Figure 7.

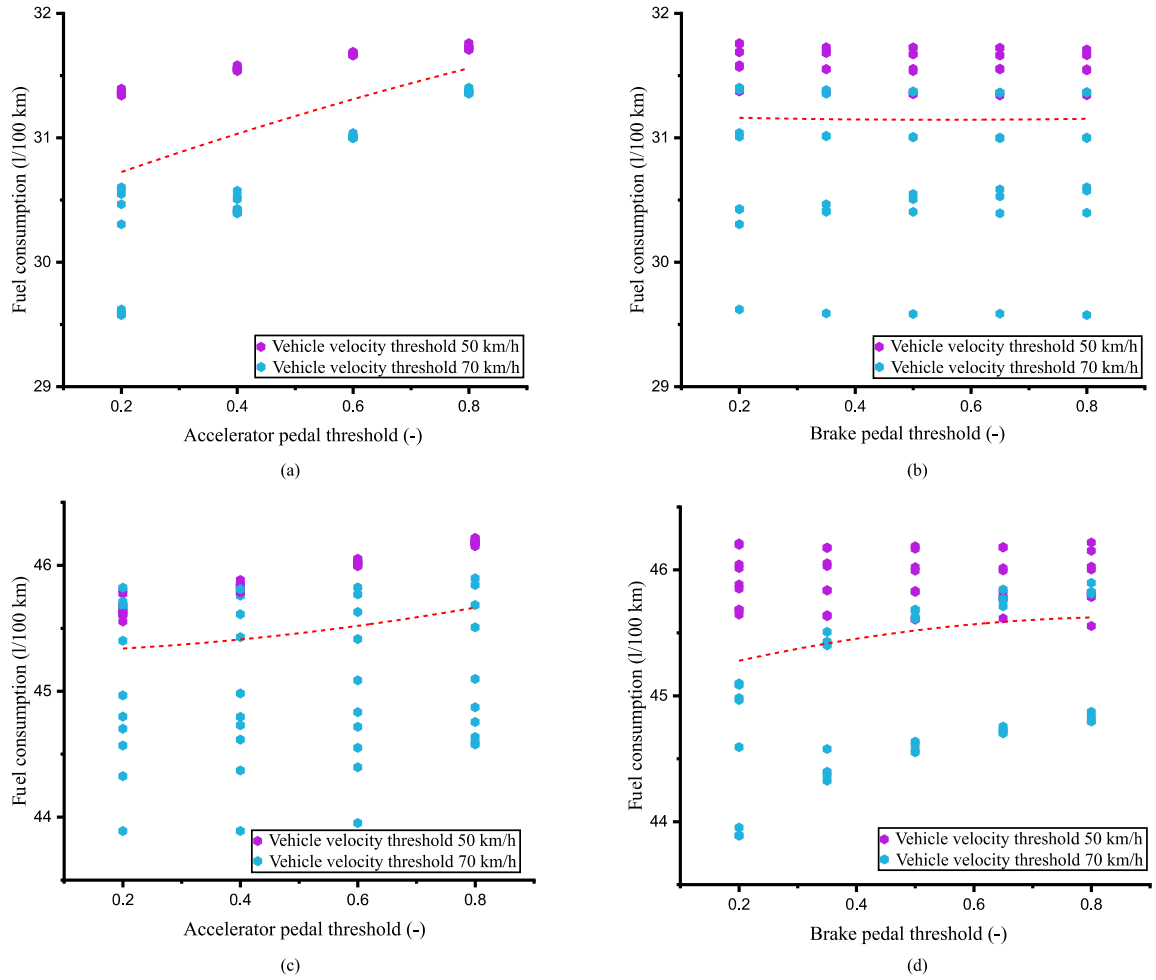

Figure 5. Fuel consumption prediction for the first driving cycle, (a) fuel consumption vs. accelerator pedal position threshold – empty scenario (b) fuel consumption vs. Brake pedal threshold – empty scenario (c) fuel consumption vs. accelerator pedal threshold – full load scenario (d) fuel consumption vs brake pedal threshold – full load scenario.

The battery SoC for the first driving cycle and both scenarios with different pedal threshold values have been depicted in Figure 7. Figure 8, shows the battery SoC for the second driving cycle with minimum fuel consumption cases. The pedals threshold values are 0.2 and 0.65 for empty scenario and 0.2 and 0.2 for the accelerator pedal and brake pedal. Compared to the results from the first driving cycle, charging mode happens more frequently due to the cycle elevation profile, especially for the full load scenario, which emphasizes the interconnection of operational conditions and control strategies. It should be noted that, while the least fuel consumption is simulated with the mentioned parameters, the end-of-cycle SoC values, except for the full-load scenario of the second driving cycle, are near the minimal SoC limit. Given the powertrain's configuration without plug-in charging capability, the end-of-cycle SoC has a substantial impact on the vehicle's subsequent cycle run. A charge-sustaining strategy should be considered for optimal control parameter definition, as it can offer a more accurate end-of-cycle SoC for comparing different configurations.

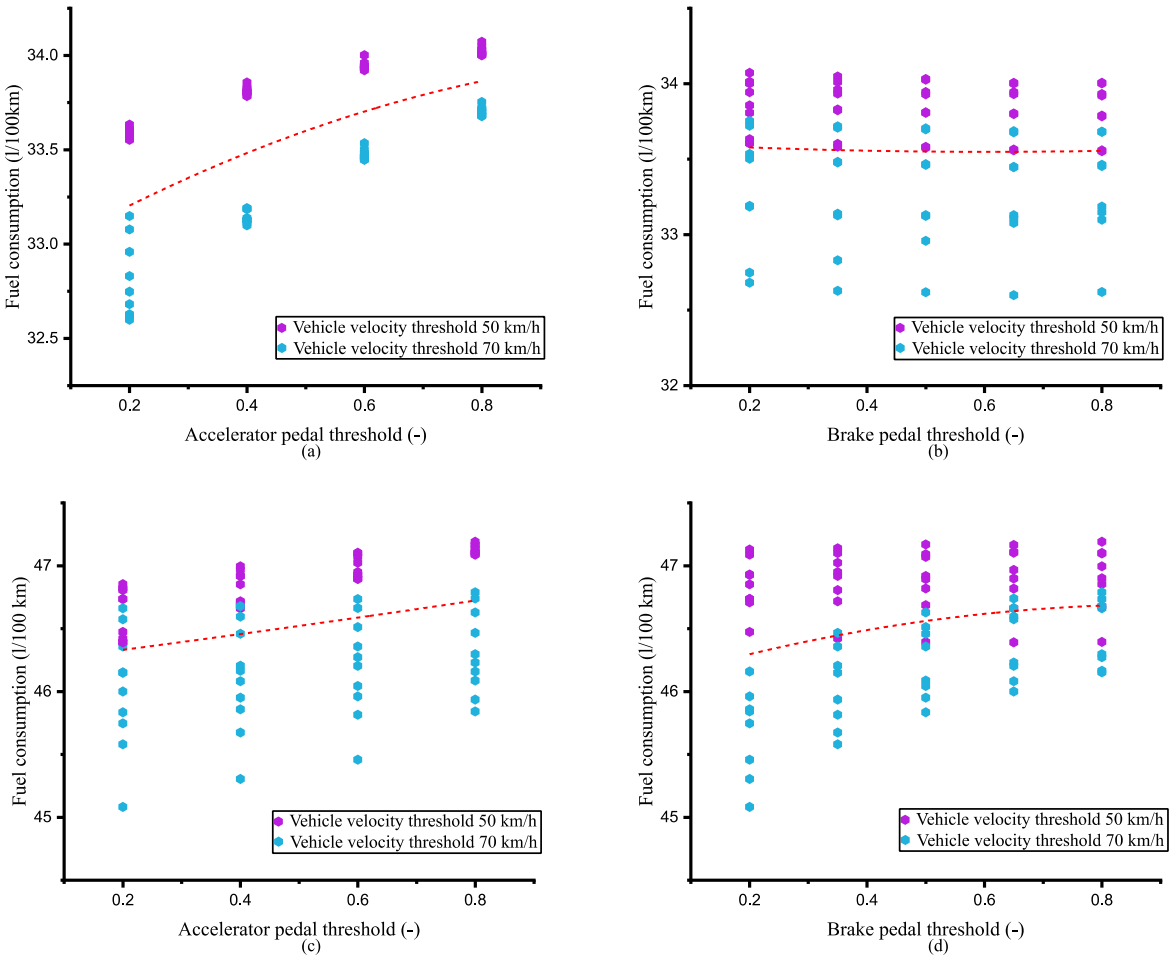

Figure 6. Fuel consumption prediction for the second driving cycle, (a) fuel consumption vs. accelerator pedal position threshold – empty scenario (b) fuel consumption vs. Brake pedal threshold – empty scenario (c) fuel consumption vs. accelerator pedal threshold – full load scenario (d) fuel consumption vs brake pedal threshold – full load scenario.

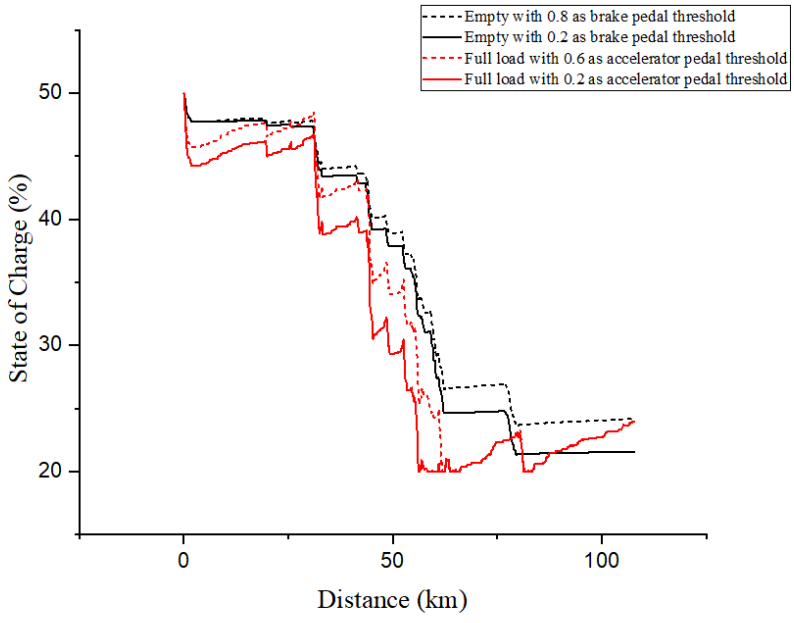

Figure 7. SoC for the best fuel consumption cases of the first driving cycle.

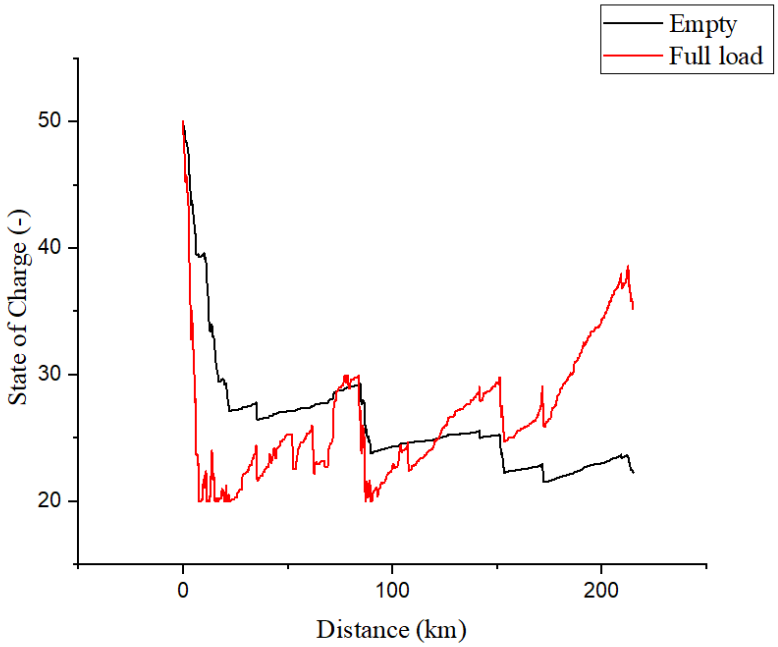

Figure 8. SoC for the best fuel consumption cases of the second driving cycle.

Driving Cycle	Battery capacity	Full load	Empty
First driving cycle	30 kWh	6.8 %	6.9 %
	15 kWh	4.7 %	4.7 %
Second driving cycle	30 kWh	6.8 %	4.2 %
	15 kWh	5.1 %	3.8 %

Table 5.Summary of fuel consumption improvement.

Table 5 presents the percentage improvement in fuel consumption achieved with the optimal control parameters for each scenario. The variations in load and driving cycles are key indicators for battery sizing. The consumption improvements for the first driving cycle are almost identical for both the full-load and empty scenarios and highly depends on the battery capacity. However, for the second driving cycle, better fuel consumption has been achieved in the full-load scenario. The state of the charge (SoC) graphs in Figure 8 indicate that the battery charge can be consumed rapidly, which emphasizes the significance of the optimizing charging mode to maximize efficiency. While the resistance forces eliminate the need for engaging brakes to keep the desired velocity in the first driving cycle and the empty scenario of the second driving cycle, due to the high load and the road altitude profile of the second driving cycle, the driver needs to use the brake more often and charge the battery subsequently. Therefore, the recovered energy from the braking improves the total fuel consumption.

4 Conclusion

This study investigates the impacts of control strategy and battery sizing on the fuel consumption of a hybridized powertrain and the influence of operational conditions on component sizing. A truck with an 8x4 axle configuration equipped with an e-axle has been simulated for two driving cycles and two load scenarios. The main conclusions of this study are as follows:

- Despite using a relatively simple control strategy, our study emphasizes the critical importance of the control unit in optimizing both component sizing and attaining optimal fuel consumption for a predetermined set of components.
- The results show the high importance of considering operational conditions for determining design parameters.
- A simulation framework is required to investigate different design criteria for each subsystem of a hybrid powertrain.

A holistic development procedure is required to design an e-axle for specific use cases, however, the development of components of an e-axle might be done by separate development teams. The developed simulation in this study will be used as a base simulation of an HDV with a P4 hybrid configuration without plug-in charging capability

to define FMUs for each subsystem and facilitate the required simulation framework. In the case of designing the e-axle as an add-on solution to an existing powertrain, a vehicle FMU, including vehicle axle configuration, ICE, and driveline, a battery FMU, including battery electric and thermal simulation; and a motor FMU, including electric motor model, are the minimum set of required FMUs. However, for higher fidelity of analysis, more details should be added to FMUs, such as auxiliary system power demand, inverter simulation, motor torque limiter, battery power demand limiter, and electric motor thermal behavior, to name a few. These features will be added to the developed simulation when the required data for simulation are available. By defining the FMU interfaces, co-simulation of different simulation tools and simulation methods will be possible which ease the cooperation between development teams. Moreover, fleet owners by defining their most common operational condition can interact with the e-axle component developer to customize suitable solutions according to their specific needs.

5 Acknowledgements

The authors would like to acknowledge to the Business Finland founded project, NoDamage (1546/31/2022), for the financial support.

6 References

[1] U. Epa and C. Change Division, “Inventory of U.S. Greenhouse Gas Emissions and Sinks: 1990-2021 – Main Report,” 1990. [Online]. Available: https://www.epa.gov/ghgemissions/inventory-us-greenhouse-gas-emissions-and-

[2] M. Ehsani, K. V. Singh, H. O. Bansal, and R. T. Mehrjardi, “State of the Art and Trends in Electric and Hybrid Electric Vehicles,” Proceedings of the IEEE, vol. 109, no. 6, pp. 967–984, Jun. 2021, doi: 10.1109/JPROC.2021.3072788.

[3] Y. Wang, A. Biswas, R. Rodriguez, Z. Keshavarz-Motamed, and A. Emadi, “Hybrid electric vehicle specific engines: State-of-the-art review,” Energy Reports, vol. 8. Elsevier Ltd, pp. 832–851, Nov. 01, 2022. doi: 10.1016/j.egyr.2021.11.265.

[4] K. V. Singh, H. O. Bansal, and D. Singh, “A comprehensive review on hybrid electric vehicles: architectures and components,” Journal of Modern Transportation, vol. 27, no. 2. Springer Berlin Heidelberg, pp. 77–107, Jun. 01, 2019. doi: 10.1007/s40534-019-0184-3.

[5] M. S. Bin Ahmad, A. Pesyridis, P. Sphicas, A. Mahmoudzadeh Andwari, A. Gharehghani, and B. M. Vaglieco, “Electric Vehicle Modelling for Future Technology and Market Penetration Analysis,” Front Mech Eng, vol. 8, Jul. 2022, doi: 10.3389/fmech.2022.896547.

[6] D. G. Barroso, Y. Yang, F. A. MacHado, and A. Emadi, “Electrified Automotive Propulsion Systems: State-of-the-Art Review,” IEEE Transactions on Transportation Electrification, vol. 8, no. 2, pp. 2898–2914, Jun. 2022, doi: 10.1109/TTE.2021.3131917.

[7] I. Banagar, A. Mahmoudzadeh Andwari, S. Mehranfar, J. Könnö, and E. Kurvinen, “Electric vehicles’ powertrain systems architectures design complexity,” Future Technology, vol. 2, no. 3, pp. 1–4, Aug. 2023, doi: 10.55670/fpll.futech.2.3.1.

[8] M. Moultak, N. Lutsey, D. H. Beijing, | Berlin, and | Brussels, “TRANSITIONING TO ZERO-EMISSION HEAVY-DUTY FREIGHT VEHICLES ACKNOWLEDGMENTS,” 2017. [Online]. Available: www.theicct.org

[9] M. Jahangir Samet, H. Liimatainen, O. P. R. van Vliet, and M. Pöllänen, “Road freight transport electrification potential by using battery electric trucks in finland and switzerland,” Energies (Basel), vol. 14, no. 4, Feb. 2021, doi: 10.3390/en14040823.

[10] S. Joshi, M. Dahodwala, E. W. Koehler, M. Franke, D. Tomazic, and J. Naber, “Trade-Off Analysis and Systematic Optimization of a Heavy-Duty Diesel Hybrid Powertrain,” in SAE Technical Papers, SAE International, Apr. 2020. doi: 10.4271/2020-01-0847.

[11] F. Salek, E. Abouelkhair, M. Babaie, F. Cunliffe, and W. Nock, “Multi-Objective Optimization of the Fuel Cell Hybrid Electric Powertrain for a Class 8 Heavy-Duty Truck,” in SAE Technical Papers, SAE International, Apr. 2023. doi: 10.4271/2023-01-0473.

[12] F. Salek, P. Halder, A. Thomas Leonard, M. Babaie, S. Resalati, and A. Zare, “Battery Sizing, Parametric Analysis, and Powertrain Design for a Class 8 Heavy-Duty Battery Electric Truck,” in SAE Technical Papers, SAE International, Apr. 2023. doi: 10.4271/2023-01-0524.

[13] C. Lacoursì and T. Härdin, “FMIGo! A runtime environment for FMI based simulation”.

[14] Modelica Association, “System Structure and Parameterization,” 2022. [Online]. Available: http://www.opensource.org/licenses/bsd-license.html

[15] Wikipedia, “Sisu Polar specificaion,” https://en.wikipedia.org/wiki/Sisu_Polar#cite_note-M-B_UK:_OM501LA_350_kW-8. Accessed: Apr. 17, 2024. [Online]. Available: https://en.wikipedia.org/wiki/Sisu_Polar#cite_note-M-B_UK:_OM501LA_350_kW-8

[16] Mercedes-Benz, “Mercedes-Benz Actros specifications,” https://www.zimoco.co.zw/wp-content/uploads/2016/10/MBSAActrosSpecificationFA1.pdf. Accessed: Apr. 17, 2024. [Online]. Available: https://www.zimoco.co.zw/wp-content/uploads/2016/10/MBSAActrosSpecificationFA1.pdf

[17] O. Delgado et al., “Fuel eFFiciency Technology in european heavy-DuTy vehicles: Baseline anD poTenTial For The 2020-2030 Time Frame,” 2017. [Online]. Available: www.theicct.org

[18] H. Eichlseder, S. Hausberger, M. Rexeis, J. Blassnegger, and G. Silberholz, “graz-vehicle simulation_Component-Certification_Delgado-Rodriguez_ICCT,” 2011.